

Grid Connected Solar Microinverter Based On Single Stage Boost Conversion

P.Jeyankondan, V.Hemamageswari, Dr. M .Santhi

Abstract— This topology represents the grid connected solar microinverter based on single stage boost conversion. This circuit can extract maximum solar power from solar panel .The output voltage of the circuit is stabilized by the use of closed loop control. Transformer gives isolation between converter circuit and inverter circuit. And also this topology reduced the number of switches needed

Index Terms— Grid connected solar microinverter.Isolated boost converter, Inverse buck converter, Maximum solar power, PV panel, Single stage boost conversion, Voltage doubler circuit.

1 INTRODUCTION

THE increasing number of renewable energy sources and distributed generators requires new strategies for the operation and management of the electricity grid in order to maintain or even to improve the power-supply reliability and quality. In addition, liberalization of the grids leads to new management structures, in which trading of energy and power is becoming increasingly important. The power-electronic technology plays an important role in distributed generation and in integration of renewable energy sources into the electrical grid, and it is widely used and rapidly expanding as these applications become more integrated with the grid-based systems.

During the last few years, power electronics has undergone a fast evolution, which is mainly due to two factors. The first one is the development of fast semiconductor switches that are capable of switching quickly and handling high powers. The second factor is the introduction of real-time computer controllers that can implement advanced and complex control algorithms. These factors together have led to the development of cost-effective and grid-friendly converters. While fossil fuel exhaustion and greenhouse effects are widely concerned around the world, one of the most important issues toward these problems is to find alternative energy for long-term solutions. Green energy offering the promise of clean and abundant energy gathered from self renewing sources such as solar energy, geothermal energy, and wind source is broadly developed. Solar cells are unique in that they directly convert the incident solar irradiation into electricity. Photovoltaic (PV) power management concepts are essential to extract as much power as possible from the solar energy. PV energy systems are being extensively studied because of their benefits of environmental friendly and renewable characteristics. Typically, several PV panels are connected in series to provide a high-voltage output.

- P.Jeyankondan is currently pursuing masters degree program in power electronics and drives in Anna University, India, E-mail: jeyaporkodi@gmail.com
- V.Hemamageswari –Assitant professor-Sethu Institute of Technology, India., E-mail: hemanthinihema@gmail.com
- Dr M. Santhi-Professor and Head Of the Department Electrical&Electronics Engineering -Sethu Institute of Technology, India.

Photovoltaic power is an established technology and has recently experienced rapid growth over the last ten years. Photovoltaic cells are the key component in most photovoltaic power systems, but their performance is still subpar, so future work is needed to improve their performance and optimize the interactions between the cells and other components. The purpose of this paper is to investigate how to improve the control of the power interface and optimize the operation of the overall system.

Photovoltaic power is an established technology and has recently experienced rapid growth over the last ten years. Photovoltaic cells are the key component in most photovoltaic power systems, but their performance is still subpar, so future work is needed to improve their performance and optimize the interactions between the cells and other components. The purpose of this paper is to investigate how to improve the control of the power interface and optimize the operation of the overall system.

2 SYSTEM DESCRIPTION

Fig. 1 shows the circuit topology of studied solar microinverter. The grid connected solar microinverter consists of isolated boost converter with a secondary voltage doublers and inverter circuit. Fig. 2 shows the modes of operation of grid connected solar microinverter with single stage boost conversion. According to the ac grid voltage the above circuit operates two modes they are explained below.

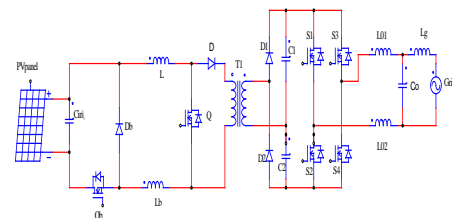
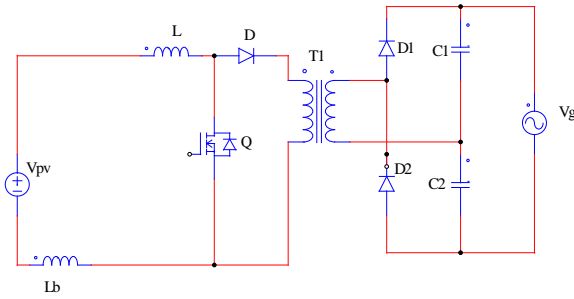


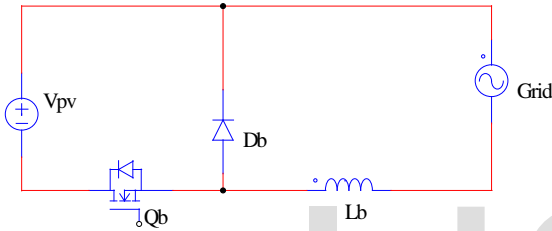
Fig.1. Circuit diagram

Mode 1: When the grid voltage is higher than a boundary voltage V_b expressed as equation (1), solar microinverter is operated under this mode

$$V_b = \frac{2n}{1 - \delta_{boost,min}} V_{pv} \quad (1)$$



(a) Mode 1



(b) Mode 2

Fig.2. Modes of operation

Where n is the turns ratio of transformer T_1 , $\delta_{boost,min}$ is the minimum duty cycle of boost switch Q and V_{pv} denotes the PV panel voltage. PV panel voltage V_{pv} is directly fed to the boost converter. Under this operation mode, the buck switch Q_b is always on the duty cycle δ_{boost} . Q is modulated as equation (2) to provide a rectified sinusoidal waveform $|V_g|$. C_1 and C_2 are connected with the AC grid system via inverter and LC output filter. Because the inverter is operated at the Zero crossing of the AC grid voltage, the switching losses are neglected. Assuming that the conduction loss on power devices of the inverse buck and inverter can be ignored, the only loss of studied solar micro inverter is due to the single stage power conversion of the isolated boost converter circuit. High conversion efficiency can thus be achieved, i.e.,

$$\delta_{boost} = 1 - \frac{2nV_{pv}}{|V_g|} \quad (2)$$

Mode 2: When the ac grid voltage is lower than the boundary voltage V_b , the solar micro inverter is operated under this mode. The duty cycle δ_{boost} of Q is fixed at the minimum value $\delta_{boost,min}$ to provide a constant voltage gain K_b as follows:

$$K_b = \frac{2nV_{pv}}{1 - \delta_{boost}} \quad (3)$$

The duty cycle δ_{buck} of buck switch Q_b is modulated as equation (4) to provide a rectified sinusoidal waveform $|V_g|$ on capacitors C_1 and C_2 that is connected with the ac grid system via inverter and LC filter, i.e.,

$$\delta_{boost} = \frac{|V_g|}{K_b V_{pv}} \quad (4)$$

Fig. 3 and Fig. 4 respectively shows the equivalent circuits of studied solar microinverter under mode 1 and mode 2.

State 1 (t_0-t_1): During this time interval, power MOSFET Q ON, and diodes D_1 and D_2 are off. The solar energy is stored into input inductor L . The load energy is provided by voltage doubler capacitors C_1 and C_2 .

State 2 (t_1-t_2): During the interval, power MOSFET Q is turned off. The solar energy stored in inductor L is released via transformer T_1 and diodes D_1, D_2 .

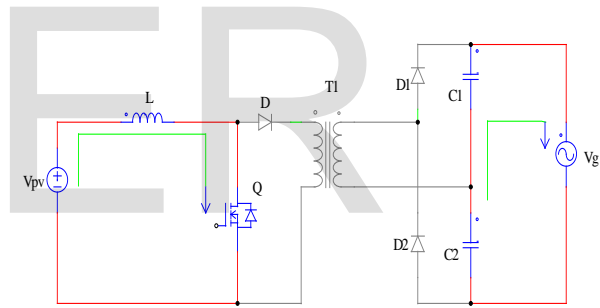
Mode 2: This mode for isolated solar microinverter can be divided into two switching states.

State 1 (t_0-t_1): During the time interval, power MOSFET Q_b is on and diode D_b is off. The solar energy is stored into buck inductor L_b . The voltage across L_b can be expressed as follows:

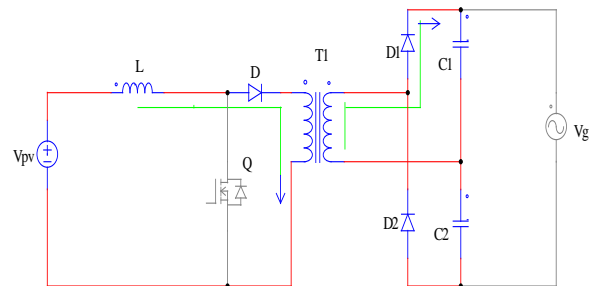
$$V_{Lb} = V_{pv} - \frac{|V_g|}{K_b} \quad (5)$$

State 2 (t_1-t_2): At t_1 , power MOSFET Q_b is turned off. The solar energy stored in buck inductor L_b is released via diode D_b . The voltage across L_b can be expressed as follows:

$$V_{Lb} = -\frac{|V_g|}{K_b} \quad (6)$$

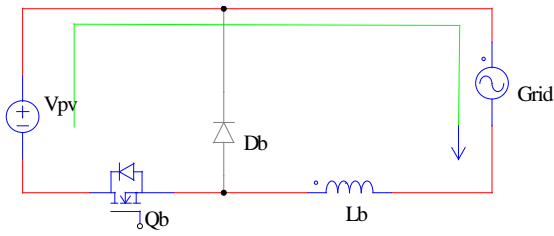


(a) Mode 1 state 1

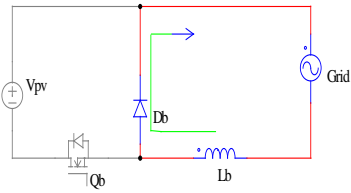


(b) Mode 1 state 2

Fig. 3. Mode 1 operating states



(a) Mode 2 State 1



(b) Mode 2 State 2

Fig.4. Mode 2 operating states

3 DESIGN CONSIDERATION

Isolated boost converter circuit

According to the waveforms shown in Fig .9 , the voltage stresses on power MOSFET Q can be represents as follows:

$$V_Q = \frac{V_{g,pk}}{n} \quad (7)$$

Where $V_{g,pk}$ denotes the peak value of the ac grid voltage. The transformer turns ratio is usually set higher than unity; therefore low voltage stresses on Q can be achieved. With low voltage stress on Q can be achieved. With low-voltage-rating devices for Q, low ON-state resistance $R_{ds(on)}$ can significantly reduce the conduction losses. The voltage stresses for diodes D_1 and D_2 and capacitors C_1 and C_2 can be determined by

$$V_{D1,D2,C1,C2} = \frac{V_{g,pk}}{2} \quad (8)$$

Considering the current ripple amount ΔIL , the inductance L can be calculated by

$$L = \frac{(|V_g|/n - V_{pv})(1 - \delta_{boost})T_s}{\Delta I_L} \quad (9)$$

Where T_s is the switching period of power MOSFET

B. Inverse-Buck Circuit

The voltage stresses on power MOSFET Q_b and diode D_b can be represented as follows:

$$V_{Qb,VDb} = V_{pv} \quad (10)$$

With low-voltage-rating devices for Q_b and D_b , high conversion efficiency can be achieved due to low conduction losses.

Considering the current ripple amount ΔIL_b , the inductance of L_b can be calculated by

$$L_b = \frac{|V_g|(1 - \delta_{buck})T_s}{K_b \Delta I_L} \quad (11)$$

where T_s is the switching period of power MOSFET Q_b .

4 SIMULATION RESULTS

The simulations were realized with a PV panel voltage of 25 V, a grid voltage of at 50 Hz and a switching Frequency of 20 KHZ. The bus capacitors were formed by two 3 mF capacitors connected in series. The output filter was formed by two inductors and a capacitor. The value of output capacitor is 2.2 mF. The output inductors values are 2.5mH. The inverter stage is formed by four (S1 to S4) switches. They are able to generate 230V, 50 HZ ac supply.

The simulation output of the PV panel. The PV panel design is simulated for 25V

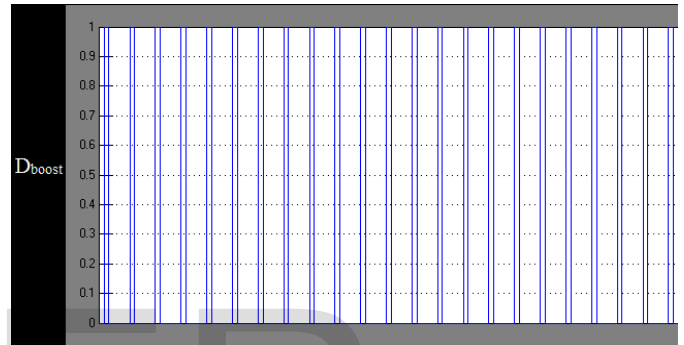


Fig.5 switching pulse for boost switch

Fig.5 shows the switching pulse of boost switch. X axis denotes the time period, Y axis denotes duty ratio.

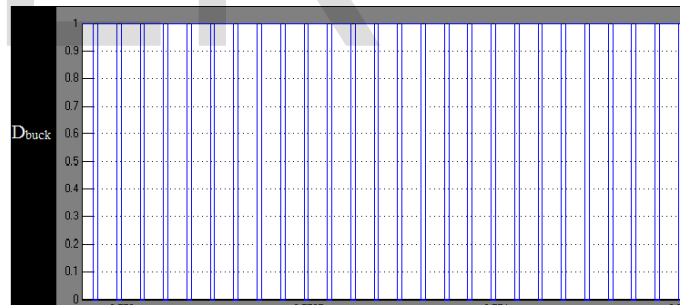


Fig.6 switching pulse for buck switch

Fig.6 shows the switching pulse of buck switch. X axis denotes the time period, Y axis denotes duty ratio.

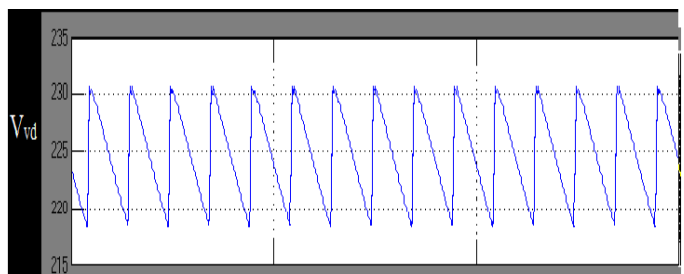


Fig.7 voltage doubler output

Fig.7 shows the simulation output of the voltage doubler output voltage. X axis denotes time period, Y axis denotes V_{vd} voltage doubler output voltage.

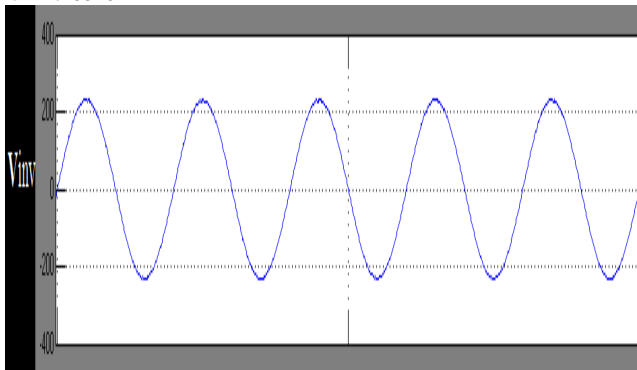


Fig.8 Inverter output

Fig.8 shows the output voltage of inverter. The inverter circuit consists of 4 switches S_1 - S_4 . Its output voltage depends on the voltage doubler output. In Y axis denote V_{inv} inverter output voltage.

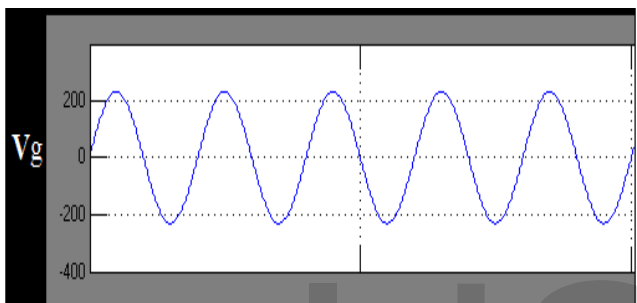
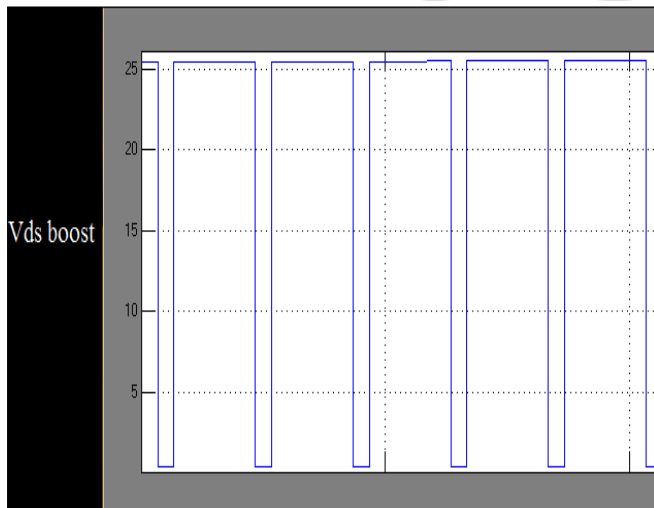


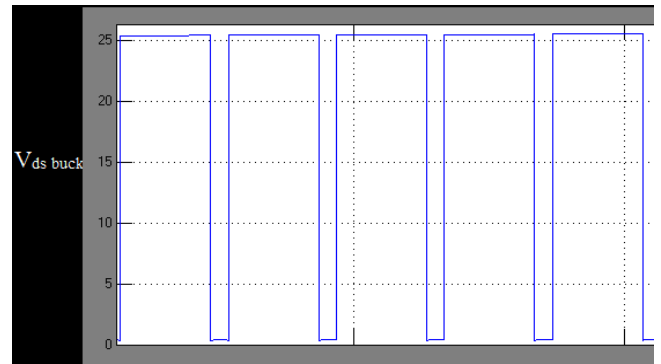
Fig .9 Grid voltage

Fig .9 shows the grid voltage of the grid connected circuit. Generally PV inverters are connected with distributed generation such as lighting loads for commercial and domestic purpose. In Y axis denotes V_g grid voltage.



(a)Boost switch

Fig.10a shows the switching pulse of the boost switch Q . In Y axis denotes $V_{ds boost}$ drain to source voltage and fig.10b shows the switching pulse of the buck switch. In Y axis denotes $V_{ds buck}$ drain to source voltage and the duty cycle of the Q and Q_b depends on the modes of operation and output voltage of the inverter.



(b) Buck switch

Fig.10 voltage across the boost and buck switches

TABLE I

LIST OF SYMBOLS

SYMBOL	DESCRIPTION
V_{pv}	Pv panel voltage
C_{in}	Input capacitor or Input capacitance
Q_b	Buck switch
L_b	Buck Inductance
L	Boost inductor
Q	Boost switch
T_1	Transformer
D_1, D_2	Voltage doubler diode
C_1, C_2	Voltage doubler capacitor
S_1-S_4	Inverter switches
L_{01}, L_{02}	Output L filter
C_0	Output C filter
L_g	Grid inductance
δ_{boost}	Duty cycle of boost switch
δ_{buck}	Duty cycle of buck switch
n	Transformation ratio of transformer
V_b	Boundary voltage
V_g	Grid voltage
K_b	Voltage gain
ΔI_L	Ripple current of inductor L
ΔI_{L_b}	Ripple current of inductor L_b

5 CONCLUSION

This topology dealt with a transformer isolated single phase grid connected microinverter for photo voltaic system. The grid connected solar microinverter based on single stage conversion circuit gives the 230V ac for 25V PV panel input voltage. This circuit stabilizes the output voltage by the feedback switching circuit. The topology reduces the number of switches required. Here the voltage doubler circuit increases the output voltage of the converter circuit. LCL filter gives the pure form of output voltage without disturbances. Thus the grid connected solar microinverter based on single stage boost conversion is simulated. Future work is focused on switching pulse generated by SPWM.

REFERENCES

- [1] [1 M. J. V. Vazquez, J. M. A. Marquez, and F. S. Manzano, "A methodology for optimizing stand-alone PV-system size using parallel-connected dc/dc converters," *IEEE Trans. Ind. Electron.*, vol. 55, no. 7, pp. 2664–2673, Jul. 2008.
- [2] J. H. Lee, H. S. Bae, and B. H. Cho, "Resistive control for a photovoltaic battery charging system using a microcontroller," *IEEE Trans. Ind. Electron.*, vol. 55, no. 7, pp. 2767–2775, Jul. 2008.
- [3] X. Weidong, N. Ozog, and W. G. Dunford, "Topology study of photovoltaic interface for maximum power point tracking," *IEEE Trans. Ind. Electron.*, vol. 54, no. 3, pp. 1696–1704, Jun. 2007.
- [4] J. H. Park, J. Y. Ahn, B. H. Cho, and G. J. Yu, "Dual-module-based maximum power point tracking control of photovoltaic systems," *IEEE Trans. Ind. Electron.*, vol. 53, no. 4, pp. 1036–1047, Jun. 2006.
- [5] M. Fortunato, A. Giustiniani, G. Petrone, G. Spagnuolo, and M. Vitelli, "Maximum power point tracking in a one-cycle-controlled single-stage photovoltaic inverter," *IEEE Trans. Ind. Electron.*, vol. 55, no. 7, pp. 2684–2693, Jul. 2008.
- [6] N. Mutoh and T. Inoue, "A control method to charge series-connected ultra electric double-layer capacitors suitable for photovoltaic generation systems combining MPPT control method," *IEEE Trans. Ind. Electron.*, vol. 54, no. 1, pp. 374–383, Feb. 2007.
- [7] . Bacciarrelli, G. Lucia, S. Saponara, L. Fanucci, and M. Forliti, "Design, testing and prototyping of a software programmable I2C/SPI IP on AMBA bus," in *Proc. Ph. D. Res. Microelectron. Electron.*, Jun. 2006, pp. 373–376.
- [8] J. T. Bialasiewicz, "Renewable energy systems with photovoltaic power generators: Operation and modeling," *IEEE Trans. Ind. Electron.*, vol. 55, no. 7, pp. 2752–2758, Jul. 2008.
- [9] M. Bertoluzzo and G. Buja, "Development of electric propulsion systems for light electric vehicles," *IEEE Trans. Ind. Informat.*, vol. 7, no. 3, pp. 428–435, Aug. 2011.
- [10] M. P. Kazmierkowski, M. Jasinski, and G. Wrona, "DSP-based control of grid-connected power converters operating under grid distortions," *IEEE Trans. Ind. Informat.*, vol. 7, no. 2, pp. 204–211, May 2011.
- [11] Y. S. Lai, C. A. Yeh, and K. M. Ho, "A family of predictive digital controlled PFC under boundary current mode control," *IEEE Trans. Ind. Informat.*, vol. 8, no. 3, pp. 448–458, Aug. 2012.
- [12] S. Dasgupta, S. N. Mohan, S. K. Sahoo, and S. K. Panda, "A plug and play operational approach for implementation of an autonomous-microgrid system," *IEEE Trans. Ind. Informat.*, vol. 8, no. 3, pp. 615–629, Aug. 2012.
- [13] H. H. Wu, A. Gilchrist, K. Sealy, and D. Bronson, "A high efficiency 5 kW inductive charger for EVs using dual side control," *IEEE Trans. Ind. Informat.*, vol. 8, no. 3, pp. 585–595, Aug. 2012.
- [14] G. Buticchi, D. Barater, E. Lorenzani, and G. Franceschini, "Digital control of actual grid-connected converters for ground leakage current reduction in PV transformerless systems," *IEEE Trans. Ind. Informat.*, vol. 8, no. 3, pp. 563–572, Aug. 2012.
- [15] Huang-Jen Chiu, *Senior Member, IEEE*, Yu-Kang Lo, *Member, IEEE*, Chun-Yu Yang, Shih-Jen Cheng, Chi-Ming Huang, Ching-Chun Chuang, Min-Chien Kuo, Yi-Ming Huang, Yuan-Bor Jean, and Yung-Cheng Huang "A Module-Integrated Isolated Solar Microinverter", *IEEE Trans. Ind. Electron.*, vol. 60, no. 2, Feb. 2013.
- [16] R. Mastromauro and M. Dell Liserre, "A control issues in single-stage photovoltaic systems: MPPT, current and voltage control," *IEEE Trans. Ind. Informat.*, vol. 8, no. 2, pp. 241–254, May 2012.
- [17] T. Hirose and H. Matsuo, "Standalone hybrid wind-solar power generation system applying dump power control without dump load," *IEEE Trans. Ind. Electron.*, vol. 59, no. 2, pp. 988–997, Feb. 2012.
- [18] S. Jiang, D. Cao, D. Y. Li, and F. Peng, "Grid-connected boost-half bridge photovoltaic micro inverter system using repetitive current control and maximum power point tracking," in *Proc. 27th Annu. IEEE (APEC)*, Feb. 2012, pp. 590–597.
- [19] R. J. Wai and C. Y. Lin, "Dual active low-frequency ripple control for clean-energy power-conditioning mechanism," *IEEE Trans. Ind. Electron.*, vol. 58, no. 11, pp. 5172–5185, Nov. 2011.
- [20] N. Femia, G. Petrone, G. Spagnuolo, and M. Vitelli, "Distributed maximum power point tracking of photovoltaic arrays: Novel approach and system analysis," *IEEE Trans. Ind. Electron.*, vol. 55, no. 7, pp. 2610–2621, Jul. 2008.
- [21] J. M. Carrasco, L. G. Franquelo, J. T. Bialasiewicz, E. Galvan, R. C. Portillo-Guisado, M. A. M. Prats, J. I. Leon, and N. Moreno-Alfonso, "Power-electronic systems for the grid integration of renewable energy sources: A survey," *IEEE Trans. Ind. Electron.*, vol. 53, no. 4, pp. 1002–1016, Jun. 2006.
- [22] A. Al Nabulsi and R. Dhaouadi, "Efficiency optimization of a DSP-based standalone PV system using fuzzy logic and dual-MPPT control," *IEEE Trans. Ind. Informat.*, vol. 8, no. 3, pp. 573–584, Aug. 2012.
- [23] B. Sahan, A. N. Vergara, N. Henze, A. Engler, and P. Zacharias, "A single stage PV module integrated converter based on a low-power current source inverter," *IEEE Trans. Ind. Electron.*, vol. 55, no. 7, pp. 2602–2609, Jul. 2008.
- [24] A. Y. Sendjaja and V. Kariwala, "Decentralized control of solid oxide fuel cells," *IEEE Trans. Ind. Informat.*, vol. 7, no. 2, pp. 163–170, May 2011.